# Delay-Independent Safe Control with Neural Networks: Positive Lur'e Certificates for Risk-Aware Autonomy

Hamidreza Montazeri<sup>1</sup>, Milad Siami<sup>1</sup>

Abstract—We present a risk-aware safety certification method for autonomous, learning-enabled control systems. Focusing on two realistic risks, state/input delays and interval-matrix uncertainty, we model the neural network (NN) controller with local sector bounds and exploit positivity structure to derive linear, delay-independent certificates that guarantee local exponential stability across admissible uncertainties. To benchmark performance, we adopt and implement a state-of-the-art IQC NN-verification pipeline. On representative cases, our positivity-based tests run orders of magnitude faster than SDP-based IQC while certifying regimes the latter cannot—providing scalable safety guarantees that complement risk-aware control.

#### I. INTRODUCTION

Autonomous systems increasingly rely on learning-enabled components [1], yet verifying closed-loop safety under realistic risks (e.g., time delays and parametric uncertainty) remains a bottleneck in deploying AI-enabled control in safety-critical applications, including autonomous vehicles, aerospace systems, and medical devices [2].

Recent advances in NN verification have produced various approaches for certifying closed-loop stability. Semidefinite programming (SDP) based methods [3], barrier function learning methods [4], among others, are presented in a survey [5]. On a notable instance, Fazlyab et al. [3] developed a comprehensive framework using quadratic constraints for safety verification, while Yin et al. [6] extended these techniques specifically for systems with NN controllers. However, these SDP-based approaches suffer from computational complexity that scales poorly with system dimension and network size [3]. Alternative verification methods have emerged from the machine learning community, including reachability analysis [7], abstract interpretation [8], and convex relaxation techniques such as CROWN [9]. While these methods excel at providing input-output bounds for NNs, they typically focus on open-loop properties and struggle to incorporate closed-loop dynamics, particularly under realistic operational conditions like delays and uncertainties [10].

Time delays are ubiquitous in networked control systems, arising from communication latencies and computational delays [11]. The stability analysis of delayed systems has a rich history in control theory [12]. However, when combined with NN controllers, the analysis becomes significantly more complex. Recent works such as [13], [14] addressed NN control of time-delay systems but relied on computationally expensive LMIs and complex control schemes. Parametric uncertainty presents another critical challenge in real-world

deployments. The combination of delays and uncertainties has been studied extensively for linear systems [15], [16], but the introduction of NN controllers creates a three-way interaction that existing methods struggle to address.

Positive systems theory offers unique analytical advantages through its structural properties [17]. Metzler matrices provide computationally efficient certificates that are often delay-independent [18]. The connection between positive systems and sector-bounded nonlinearities through Lur'e systems has been established [19], but its application to NN verification remains underexplored [20].

This paper bridges the gap between positive systems theory and NN verification by developing a novel framework that exploits positivity constraints for efficient safety certification. Our key contributions are:

- 1) Local Sector Bounds for FFNNs: We develop a novel sector bound for feedforward NNs that, unlike existing elementwise bounds (CROWN, IBP), provides network-level sector descriptions suitable for Lur'e system analysis.
- 2) Positivity-Based Verification Framework: We introduce a scalable, delay-independent certificate that leverages Metzler matrix and positive system properties to verify NN feedback loops under both time delays and interval uncertainties.
- **3) Comprehensive Risk Analysis:** We provide unified treatment of three risk configurations: (i) interval uncertainty only, (ii) time delays only, and (iii) combined delays and uncertainties, demonstrating that our approach handles all cases with a single, computationally efficient framework.
- **4) Comparative Evaluation**: We develop and adapt the state-of-the-art IQC-based verification method for NN feedback loops to our specific risk setting and use it as a baseline. We benchmark our method against this IQC baseline, demonstrating orders-of-magnitude speedups and certification in regimes where SDP-based approaches fail.

The significance of this work extends beyond theoretical contributions. As autonomous systems increasingly operate in uncertain, networked environments, the ability to efficiently certify safety under realistic operational conditions becomes paramount. Our positivity-based approach offers a path toward real-time, online verification that could enable adaptive safety certificates and risk-aware control strategies.

#### A. Notation

We denote by  $\mathbb{R}^n_+$  and  $\mathbb{R}^{n\times m}_+$  vectors and matrices with nonnegative real entries. The orders  $\geq$ , > denote the elementwise inequality for vectors and matrices of the same size, while  $\prec$ ,  $\preceq$  is used in the definiteness sense. A square matrix is Metzler if its off-diagonal entries are nonnegative.

<sup>&</sup>lt;sup>1</sup> Department of Electrical & Computer Engineering, Northeastern University, Boston, MA 02115, USA. (e-mails: {montazerihedesh.h, m.siami}@northeastern.edu).

#### II. PROBLEM STATEMENT AND MOTIVATION

## A. Problem Description

We study the stability of an autonomus AI-enabled system under two sources of risk, namely, delay and interval uncertainty. We model the system in the form of a classical Lur'e system where a static NN is in the feedback loop of a linear time invariant (LTI) plant subjected to interval uncertainty and state and input delay written in the form:

$$\dot{x}(t) = [\underline{A}_0, \overline{A}_0] x(t) + \sum_{i=1}^{\ell} [\underline{A}_i, \overline{A}_i] x(t - \tau_i) + B_i u(t - \tau_i),$$

$$y(t) = Cx(t), \qquad u(t) = \Phi(y(t)). \tag{1}$$

Here,  $A_0, A_i \in \mathbb{R}^{n \times n}$  are constant and lie in the elementwise intervals  $[\underline{A}_0, \overline{A}_0]$  and  $[\underline{A}_i, \overline{A}_i]$ ;  $B_i \in \mathbb{R}^{n \times m}$  and  $C \in \mathbb{R}^{p \times n}$  are the input and output matrices; and  $x(t) \in \mathbb{R}^n$ ,  $u(t) \in \mathbb{R}^m$ ,  $y(t) \in \mathbb{R}^p$  denote the state, input, and output, with initial state  $x(0) \coloneqq x_0$ . Assume an initial history  $x_{h_i}(t)$  on  $t \in [-\tau_i, 0]$  so all delayed terms are well-defined. The controller is a static nonlinear mapping  $\Phi : \mathbb{R}^p \to \mathbb{R}^m$  with  $\Phi(0) = 0$  rendering the origin (x, u) = (0, 0) to be equilibrium. The function  $\Phi$  is realized by a q-layer FFNN with the following equations:

$$\nu^{(1)} = W^{(1)}y + b^{(1)}, \qquad \omega^{(1)} = \varphi^{(1)}(\nu^{(1)}),$$

$$\nu^{(i)} = W^{(i)}\omega^{(i-1)} + b^{(i)}, \quad \omega^{(i)} = \varphi^{(i)}(\nu^{(i)}), \quad i = 2, \dots, q,$$

$$u = W^{(q+1)}\omega^{(q)} + b^{(q+1)}.$$
(2)

Dimensions are  $W^{(i)} \in \mathbb{R}^{n_i \times n_{i-1}}$  and  $b^{(i)} \in \mathbb{R}^{n_i}$ , with the dimensions of the first and last layers being fixed to the dimensions of system's input and output. Each activation  $\varphi^{(i)}(\cdot)$  acts elementwise and is assumed to be monotone on a prescribed interval. Most widely used activation functions satisfy the requirement. We analyze the equilibrium at the origin by enforcing  $\Phi(0) = 0$  either by design,  $b^{(i)} = 0$ , or by shifting coordinates around the operating point. The set  $(x^*, u^*, \nu^*, \omega^*)$  denotes the equilibrium states.

## B. Challenges and Why Existing Methods Fall Short

The closed loop system in (1) is a complex nonlinear system with three coupled sources of uncertainty/nonlinearity, namely time delay, interval matrices, and an NN controller, making safety verification challenging. Standard nonlinear analysis reduces the problem to large SDPs to certify delay/uncertainty margins. Inserting an NN further inflates these LMIs with auxiliary variables and multipliers. Feasibility is also highly sensitive to the specific delay and uncertainty values, so the SDP must be re-solved whenever these parameters change. As a result, SDP-based approaches become computationally intractable at scale [3]. Even LMI-free analytic results for linear systems are delay-dependent and do not extend gracefully to additional uncertainties or nonlinear (NN) feedback. We later illustrate these limitations on representative examples and explanatory notes.

In response, we develop a positivity-based verification framework for (1). We wrap the NN in a tailored sector bound that enforces positivity of the feedback interconnection, and then

leverage tools from positive-systems theory. The outcome is a delay-independent, highly scalable method for safety verification of NN feedback loops.

## III. PRELIMINARIES AND BACKGROUND

A. Positive Systems

Consider an LTI system of the form:

$$\dot{x}(t) = Ax(t) + Bu(t), \quad y(t) = Cx(t), \tag{3}$$

**Definition 1.** The system in (3) is called "internally positive" if,  $\forall t > 0$ , we have  $x(t) \geq 0$ , given  $x_0 \geq 0$  and  $u(t) \geq 0$ .

**Lemma 1.** The system in (3) is internally positive if and only if A is a Metzler matrix,  $B \in \mathbb{R}_+^{n \times m}$ , and  $C \in \mathbb{R}_+^{p \times n}$ . If the internally positive system is also asymptotically stable, then there exists a vector  $v \in \mathbb{R}_+^n$ , with v > 0, such that  $v^{\top}A < 0$ .

Consider the delayed linear system

$$\dot{x}(t) = A_0 x(t) + \sum_{i=1}^{l} A_i x(t - \tau_i) + B_i u(t - \tau_i), \quad y(t) = C x(t),$$
(4)

**Lemma 2.** The system (4) is internally positive if and only if  $A_0$  is a Metzler matrix and  $A_i \in \mathbb{R}^{n \times n}_+; B_i \in \mathbb{R}^{n \times m}_+, C \in \mathbb{R}^{p \times n}_+$  are nonnegative matrices.

The preceding definitions and lemmas are presented in foundational references on positive systems, e.g., [17], and in subsequent developments such as [18, Lem. 1].

#### B. NN Sector Bounds

**Definition 2** ( $\Gamma$ -Sector Bounded Function). Given an interval  $[\Sigma_1, \Sigma_2]$  with  $\Sigma_1, \Sigma_2 \in \mathbb{R}^{m \times p}$  and  $\Sigma_1 \leq \Sigma_2$ , a static nonlinear function  $\Phi(y) : \mathbb{R}^p \to \mathbb{R}^m$  is said to be  $\Gamma$ -sector bounded within that interval if, for a compact and connected set  $\Gamma \subseteq \mathbb{R}^p$ , the following condition holds:

$$\Sigma_1 y \le \Phi(y) \le \Sigma_2 y, \quad \forall y \in \Gamma \subset \mathbb{R}^p.$$
 (5)

Interval Arithematic: To apply the local sector bounds, we first need to compute box bounds on each pre-activation  $\nu^{(i)}$ . These boxes are calculated by propagating the input once in the forward path of the network. Initialize at the first layer by selecting an interval  $[\underline{\nu}^{(1)}, \overline{\nu}^{(1)}]$  containing the equilibrium  $\nu_*^{(1)}$ . Monotonic activations map intervals elementwise, e.g., if  $\nu \in [\underline{\nu}, \overline{\nu}]$ , then  $\phi(\nu) \in [\phi(\underline{\nu}), \phi(\overline{\nu})]$ , yielding  $[\underline{\omega}^{(1)}, \overline{\omega}^{(1)}]$ . For the next layer, the ith coordinate  $(\nu_i^{(2)} = W_{i,:}^{(2)}\omega^{(1)} + b_i^{(2)})$  satisfies

$$\overline{\nu}_i^{(2)} = \max_{\underline{\omega}^{(1)} \leq \underline{\omega}^{(1)} \leq \overline{\omega}^{(1)}} \nu_i^{(2)}, \qquad \underline{\nu}_i^{(2)} = \min_{\underline{\omega}^{(1)} \leq \underline{\omega}^{(1)} \leq \overline{\omega}^{(1)}} \nu_i^{(2)},$$

where  $W_{i,:}$  is the ith row of W. Let  $c:=\frac{1}{2}(\overline{\omega}^{(1)}+\underline{\omega}^{(1)})$  and  $r:=\frac{1}{2}(\overline{\omega}^{(1)}-\underline{\omega}^{(1)})$ . Since the objective is linear over the box  $[\underline{\omega}^{(1)},\overline{\omega}^{(1)}]$ , these programs have the closed forms

$$\overline{v}_i^{(2)} = W_{i,:}^{(2)}c + b_i^{(2)} + |W_{i,:}^{(2)}|\,r, \quad \underline{v}_i^{(2)} = W_{i,:}^{(2)}c + b_i^{(2)} - |W_{i,:}^{(2)}|\,r.$$

Thus  $\nu^{(2)} \in [\underline{\nu}^{(2)}, \overline{\nu}^{(2)}]$ . Repeating this propagation layer-by-layer provides  $[\underline{\nu}^{(i)}, \overline{\nu}^{(i)}]$  for all layers, which we then use to form the local sector bounds.

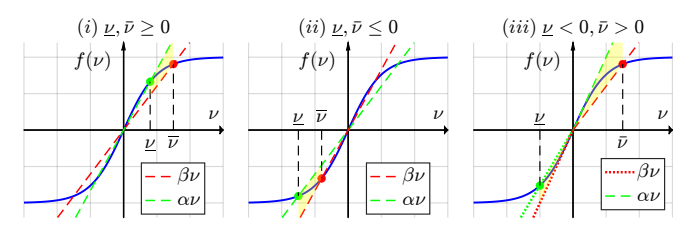


Fig. 1: Sector relaxations of  $\phi(\nu) = \tanh(\nu)$ : (i)  $\beta\nu \le \tanh(\nu) \le \alpha\nu$ :  $\beta = \tanh(\overline{\nu})/\overline{\nu}$ ,  $\alpha = \tanh(\underline{\nu})/\underline{\nu}$ . (ii)  $\beta\nu \le \tanh(\nu) \le \alpha\nu$   $\beta = \tanh(\overline{\nu})/\overline{\nu}$ ,  $\alpha = \tanh(\underline{\nu})/\underline{\nu}$ . (iii)  $-\beta|\nu| \le \tanh(\nu) \le \alpha|\nu|$  with  $\beta = \alpha = \tanh'(0) = 1$ .

## IV. MAIN RESULTS

This section is organized into three interconnected subsections. First, we develop a *local sector bound* for FFNNs, providing the analytical machinery and notation used throughout the sequel. Building on this foundation, the second subsection introduces a *positivity-based verification* framework, leveraging the sector bounds and positive systems theory to obtain delay and uncertainty-robust certificates. The third subsection then presents an *IQC-based verification* method formulated to utilize the state-of-the-art NN-in-the-loop analysis pipelines presented in [6] for our specific system; beyond furnishing an alternative certificate, this construction is used to assemble a strong benchmark against which we systematically compare our proposed method.

#### A. Local Sector Bounds for FFNNs

Our analysis requires a network-level sector bound for the entire NN, whereas existing bounds in the literature (e.g., CROWN, IBP, BERN-NN) generally yield elementwise or layerwise affine enclosures that do not match the required sector geometry. Accordingly, in this section we develop a novel sector bound for FFNNs. The construction follows the standard convex-relaxation pipeline popular in ML verification bounds, but replaces the usual affine envelopes with a tailored sector relaxation of the activation functions, which is then propagated through the network to produce a  $[\gamma_1, \gamma_2]$  sector bound. Consider the FFNN in (2) with fixed weight/bias and input y restricted to the componentwise box  $\Gamma := \{y \in \mathbb{R}^{n_0}_+: y \leq y \leq \overline{y}, y \neq 0^1\}$ .

Step A: propagation through weights and biases

Assume the post-activation vector of layer i satisfies

$$\ell^{(i)}y \le \omega^{(i)} \le u^{(i)}y, \tag{6}$$

with initialization  $\ell^{(0)}=u^{(0)}=I_{n_0}$ . For the next preactivation  $\nu=W\omega+b$ , split  $W=W^++W^-$  with  $W^+_{ij}=\max\{W_{ij},0\}$  and  $W^-_{ij}=\min\{W_{ij},0\}$ , and set

$$\underline{\sigma} = W^+ \ell + W^- u, \qquad \overline{\sigma} = W^+ u + W^- \ell.$$
 (7)

Then

$$\sigma y \leq W \omega \leq \overline{\sigma} y.$$
 (8)

<sup>1</sup>Since the application of the bound is in positive systems regime, usually  $y \in \mathbb{R}^{n_0}_+$ . Moreover, setting biases to zero will waive the requirement  $y \neq 0$ .

For the bias, let  $a_1 := \min_k \underline{y}_k$  and  $a_2 := \max_k \overline{y}_k$ , and define  $\delta, \overline{\delta} \in \mathbb{R}^{n_i \times n_0}$  rowwise by

$$\underline{\delta}_{j} = \begin{cases} b_{j}/a_{2} & b_{j} \ge 0 \\ b_{j}/a_{1} & b_{j} < 0 \end{cases}, \qquad \overline{\delta}_{j} = \begin{cases} b_{j}/a_{1} & b_{j} \ge 0 \\ b_{j}/a_{2} & b_{j} < 0 \end{cases}. \tag{9}$$

Thus,  $\underline{\delta}_i y \leq b \leq \overline{\delta}_j y$ . Combining (8)–(9) yields

$$L^{(i+1)}u < \nu^{(i+1)} = W^{(i+1)}\omega^{(i)} + b^{(i+1)} < U^{(i+1)}u.$$
 (10)

with  $L := \underline{\sigma} + \underline{\delta}$  and  $U := \overline{\sigma} + \overline{\delta}$ . This preserves the linear-in-y sector form layer by layer.

### Step B: Activation relaxation

We convert  $\omega^{(i)} = \phi(\nu^{(i)})$  into linear sector bounds depending on the box of preactivation  $[\underline{\nu}^i, \overline{\nu}^i]$  calculated by the interval arithmetic explained in subsection III-B. Assume the pre-activation of layer i obeys

$$L^{(i)}y \le \nu^{(i)} \le U^{(i)}y,$$
 (11)

as shown in (10). For neuron j, let  $\underline{\nu}_j^{(i)}$  and  $\overline{\nu}_j^{(i)}$  be the corresponding entries of the preactivation box  $[\underline{\nu}^i, \overline{\nu}^i]$ . On the interval  $[\underline{\nu}_j^{(i)}, \overline{\nu}_j^{(i)}]$ , define slopes  $(\alpha_j^{(i)}, \beta_j^{(i)})$  so that  $\beta_j^{(i)} \nu_j^{(i)} \leq \phi(\nu_j^{(i)}) \leq \alpha_j^{(i)} \nu_j^{(i)}$ .

$$(\mathbf{i}) \ \ \mathrm{if} \ \underline{\nu}, \overline{\nu} \geq 0: \qquad \qquad \beta_j^{(i)} = \frac{\phi(\overline{\nu})}{\overline{\nu}}, \ \alpha_j^{(i)} = \frac{\phi(\underline{\nu})}{\nu};$$

(ii) if 
$$\underline{\nu}, \overline{\nu} \leq 0$$
:  $\beta_j^{(i)} = \frac{\phi(\overline{\nu})}{\overline{\nu}}, \ \alpha_j^{(i)} = \frac{\phi(\underline{\nu})}{\nu};$ 

(iii) if 
$$\underline{\nu} \le 0, \overline{\nu} \ge 0$$
:  $\beta_j^{(i)} = \alpha_j^{(i)} = \sup_{\nu \ne 0} |\phi(\nu)|/|\nu|$ .

This calculation is visualized for  $\phi = \tanh$  in Fig. 1. Gather the neuronwise slopes into diagonal matrices

$$\underline{D}^{(i)} := \operatorname{diag}(\beta_j^{(i)}), \quad \overline{D}^{(i)} := \operatorname{diag}(\alpha_j^{(i)}), \tag{12}$$

and define "shape" matrices by row replacement to handle the sign-crossing case (iii):

$$\hat{L}_{j,:}^{(i)} := \begin{cases} L_{j,:}^{(i)} & \text{case } (i), (ii) \\ -|L_{j,:}^{(i)}| & \text{case } (iii), \end{cases} \quad \hat{U}_{j,:}^{(i)} := \begin{cases} U_{j,:}^{(i)} & \text{case } (i), (ii) \\ |U_{j,:}^{(i)}| & \text{case } (iii). \end{cases}$$

Then the post-activation is bounded by

$$\underline{D}^{(i)}\,\hat{L}^{(i)}\,y\,\leq\,\phi(\nu^{(i)})\,\leq\,\overline{D}^{(i)}\,\hat{U}^{(i)}\,y,\qquad\forall\,y\in\Gamma.\tag{14}$$

Network-level sector bound

Recursing Steps A–B from input to output yields a single local sector for the whole network.

**Theorem 1** (Local Sector Bound for FFNN). Consider an FFNN as in (2). For any  $y \in \Gamma = [\underline{y}, \overline{y}] \in \mathbb{R}^p_+$ , the NN mapping  $\Phi(y)$  satisfies

$$\gamma_1 y \leq \Phi(y) \leq \gamma_2 y, \tag{15}$$

$$\gamma_1 = L^{(q+1)} \left( \prod_{i=1}^q \underline{D}^{(i)} \hat{L}^{(i)} \right), \quad \gamma_2 = U^{(q+1)} \left( \prod_{i=1}^q \overline{D}^{(i)} \hat{U}^{(i)} \right),$$

where  $L^{(i)}, U^{(i)}$  come from (10), and  $\underline{D}^{(i)}, \overline{D}^{(i)}, \hat{L}^{(i)}, \hat{U}^{(i)}$  from (12)–(13).

In this section, we utilize local sector bounds and positivity constraint on systems to develop a scalable delay-independent method for verification of NN feedback loops.

**Assumption 1.**  $\underline{A}_0$  is Metzler and  $B_i, C \geq 0$ .

**Lemma 3.** Suppose Assumption 1 holds for system (1), and the feedback nonlinearity  $\Phi$  is  $\Gamma$ -sector bounded in  $[\Sigma_1, \Sigma_2]$ . Then the Lur'e system (1) is internally positive in  $\Gamma$ , if and only if  $\underline{A}_i + B_i \Sigma_1 C \geq 0$ .

*Proof.* To avoid notational complexity, we present the proof for a single delay channel ( $\ell = 1$ ), however, the argument extends unchanged to multiple channels.

Necessity. Suppose  $\Phi(Cx(t-\tau))=\Sigma_1Cx(t-\tau)$  which belongs to Sector $[\Sigma_1,\Sigma_2]$ . In this case, the closed-loop system reduces to an LTI system with dynamics  $A_0x(t)+[A_1+B\Sigma_1C]\,x(t-\tau)$ . If the Lur'e system is positive for all admissible nonlinearities and all admissible  $A_0$  and  $A_i$ , it must, in particular, be positive for the linear case  $\underline{A}_0x(t)+[\underline{A}_1+B\Sigma_1C]\,x(t-\tau)$ . As stated in Lemma 2, positivity of a delayed linear system requires the system matrix  $\underline{A}_0$  to be Metzler and  $\underline{A}_1+B\Sigma_1C\geq 0$ ; therefore, the necessity follows.

Sufficiency. Suppose that  $\underline{A}_0$  is Metzler,  $\underline{A}_1 + B\Sigma_1 C \geq 0$ , and  $\Phi \in \operatorname{Sector}[\Sigma_1, \Sigma_2]$ . Consider the j-th component of the state equation:

$$\begin{split} \dot{x}_{j}(t) &= A_{0_{jj}} x_{j}(t) + A_{1_{jj}} x_{j}(t-\tau) + \\ \sum_{k=1, k \neq j}^{n} A_{0_{jk}} x_{k}(t) + A_{1_{jk}} x_{k}(t-\tau) + (B\Phi(Cx(t-\tau)))_{j}. \end{split}$$

Assume  $x(0), x_{h,1} \in \mathbb{R}_+^n$  and suppose, for contradiction, that some component  $x_j(t)$  becomes negative. Therefore, continuity of solutions suggests that there exists a first time  $t_1 \geq 0$  such that  $x_j(t_1) = 0$ , with  $x_k(t_1) \geq 0$  for all  $k \neq j$  and  $Cx(t-\tau) \geq 0$  for  $t \in [-\tau, t_1]$ . By the sector condition, partially ordered sets, and nonnegativity of B, we obtain:

$$\dot{x}_j(t_1) \ge \underline{A}_{0_{jj}} x_j(t_1) + (\underline{A}_1 + B\Sigma_1 C)_{jj} x_j(t_1 - \tau) + \sum_{k=1, k \ne j}^n \underline{A}_{0_{jk}} x_k(t_1) + (\underline{A}_1 + B\Sigma_1 C)_{jk} x_k(t_1 - \tau).$$

Since  $x_j(t_1)=0$ ,  $\underline{A}_0$  is Metzler,  $\underline{A}_1+B\Sigma_1C\geq 0$ , and  $x_k(t)\geq 0$ , it follows that  $\dot{x}_i(t_1)\geq 0$ , contradicting the assumption that  $x_j$  becomes negative. Hence, the trajectory remains in  $\mathbb{R}^n_+$  for all  $t\geq 0$ .

For analysis purpose we consider three risk configurations:

- (C1) Interval uncertainty, no delay: the plant has interval (elementwise) parameter uncertainty and no time delays.
- (C2) **Delay only:** constant time delays in the state and input channels, with no parametric uncertainty.
- (C3) **Combined case:** simultaneous interval (elementwise) uncertainty and state/input time delays.

C1 - Interval Uncertainty, No Delay NN Feedback Loops Here we consider the system (1) with  $\tau_i = 0$ :

$$\dot{x}(t) = [\underline{A}_0, \overline{A}_0] x(t) + \sum_{i=1}^{\ell} [\underline{A}_i, \overline{A}_i] x(t) + B_i \Phi(Cx(t)), \quad (16)$$

**Theorem 2.** Consider the system (16) with the nonlinear feedback characterized by an FFNN as in (2) which is  $\Gamma$ -sector bounded in  $[\gamma_1, \gamma_2]$ . Under assumption 1, the NN feedback loop is locally exponentially stable in the set  $\Gamma$  if  $\underline{A} + B\gamma_1 C$  is Metzler and  $\overline{A} + B\gamma_2 C$  is Hurwitz, where  $\overline{A} = \sum_{i=0}^{l} \overline{A}_i, \underline{A} = \sum_{i=0}^{l} \underline{A}_i$ , and  $\gamma_1, \gamma_2$  are calculated using (15).

*Proof.* Assume  $x_0 \geq 0$ . Given  $\dot{x} \geq \underline{A} + B\gamma_1 C$ , by Lemma 3 (with no delay channel), the Metzler condition on  $\underline{A} + B\gamma_1 C \geq 0$  ensures  $x(t) \geq 0$  for all  $t \geq 0$ . Define  $M := \overline{A} + B\gamma_2 C$ , which is Hurwitz and Metzler due to the Metzler lower sector. By Lemma 1, there exists a positive vector v > 0 and scalar  $\varepsilon > 0$  such that  $v^\top M \leq -\varepsilon v^\top$ .

Consider the Lyapunov function  $V(x) = v^{\top}x$ . Since v > 0 and  $x(t) \ge 0$ , we have V(x) > 0 for all  $x \ne 0$  and V(0) = 0. Computing the time derivative along system trajectories:

$$\dot{V}(x) = v^{\top} \dot{x} = v^{\top} \left[ Ax(t) + B\Phi(Cx(t)) \right] \le v^{\top} Mx.$$

Therefore  $\dot{V}(x) \leq v^{\top} M x \leq -\varepsilon v^{\top} x = -\varepsilon V(x)$ . This implies  $V(x(t)) \leq V(x(0)) e^{-\varepsilon t}$ , establishing local exponential stability in  $\Gamma$ .

C2 - Delayed Only NN feedback loops

**Theorem 3.** Consider the delayed Lur'e system

$$\dot{x}(t) = A_0 x(t) + \sum_{i=1}^{\ell} A_i x(t - \tau_i) + B_i \, \Phi(C x(t - \tau_i)), \quad (17)$$

where the feedback  $\Phi(Cx)$  is characterized by an FFNN as in (2). Suppose there exists a local  $\Gamma$ -set including the origin in which  $\Phi(Cx)$  is sector bounded in  $[\gamma_1, \gamma_2]$ . Assume (I) (Internal positivity at the lower sector)  $A_0$  is Metzler,  $B, C \geq 0$ , and  $A_i + B\gamma_i C \geq 0$ .

(II) (Upper-sector DC Hurwitz) The DC matrix at the upper sector  $H := \sum_{i=0}^{n} A_i + B\gamma_2 C$  is Hurwitz.

Then, for every delay  $\tau \geq 0$  the closed-loop system (17) is a positive system on  $\mathbb{R}^n_+$  and is locally exponentially stable from nonnegative histories.

*Proof.* For notational simplicity, we present the proof for a single delay channel ( $\ell=1$ ); the extension to multiple channels follows analogously.

*Positivity.* The positivity of the nonlinear closed loop system follows from Lemma 3 by fixing  $A_0$  and  $A_1$ .

stability certificate. Since H is Hurwitz and Metzler (from condition (I)), there exists a positive vector v>0 and scalar  $\varepsilon>0$  such that

$$H^{\top}v < -\varepsilon v. \tag{18}$$

Assume the function  $V(x) = v^{\top}x$ . Let  $M := A_1 + B\gamma_2 C \ge 0$  and  $w^{\top} := v^{\top}M \ge 0$ . Along positive trajectories of (17), using the upper sector bound inside the derivative estimate.

$$\dot{V}(t) = v^{\top} A_0 x(t) + v^{\top} A_1 x(t-\tau) + v^{\top} B \Phi(Cx(t-\tau))$$

$$\leq v^{\top} A_0 x(t) + v^{\top} (A_1 + B\Sigma_2 C) x(t-\tau)$$

$$= v^{\top} H x(t) - w^{\top} x(t) + w^{\top} x(t-\tau)$$

$$< -\varepsilon V(t) - w^{\top} x(t) + w^{\top} x(t-\tau), \tag{19}$$

where the last inequality uses (18) and positivity of  $x(\cdot)$ . Define  $\beta := \max_j \frac{(M^\top v)_j}{v_j}$ . Thus,

$$w^{\top} x \le \beta V(x), \quad \forall x \in \mathbb{R}^n_+.$$
 (20)

Introduce the copositive Lyapunov-Krasovskii functional

$$W(t) := V(x(t)) + \int_{t-\tau}^{t} w^{\top} x(s) ds \ge 0.$$

Differentiating and using (19) yields

$$\dot{W}(t) = \dot{V}(t) + w^{\top} x(t) - w^{\top} x(t - \tau) \le -\varepsilon V(t).$$

As a result, the stability is guaranteed. To prove exponential decay, we use (20) to write

$$W(t) \le V(x(t)) + \beta \tau \sup_{u \in [t-\tau,t]} V(x(u)).$$

At times when  $V\big(x(t)\big) = \sup_{u \in [t-\tau,t]} V\big(x(u)\big)$  (which hold on a dense set by continuity), we have  $W(t) \leq (1+\beta\tau)\,V\big(x(t)\big)$ , hence

$$\dot{W}(t) \leq -\varepsilon V(t) \leq -\frac{\varepsilon}{1+\beta\tau} W(t).$$

Therefore,  $W(t) \leq W(0) \exp\left(-\frac{\varepsilon}{1+\beta\tau}t\right) \quad \forall t \geq 0$ , and consequently  $V(x(t)) \to 0$  exponentially. Since the system is positive, this implies exponential stability from nonnegative histories inside  $\Gamma$ -set for every  $\tau > 0$ .

# C3 - Delayed uncertain NN feedback loops

In the third case we combine the previous two sections and their results.

**Theorem 4.** Consider the delayed Lur'e system

$$\dot{x}(t) = \left[\underline{A}_0, \bar{A}_0\right] x(t) + \sum_{i=1}^{l} \left[\underline{A}_i, \bar{A}_i\right] x(t - \tau_i) + B_i \Phi(Cx(t - \tau_i))$$

(I) (Sector on the positive cone) Assume there exists a local  $\Gamma$ -set including the origin in which the NN  $\Phi(Cx)$  is sector bounded in  $[\gamma_1, \gamma_2]$ .

(II) (Internal positivity at the lower endpoint)  $\underline{A}_0$  is Metzler,  $B, C \geq 0$ , and  $\underline{A}_1 + B\gamma_1 C \geq 0$ .

(III) (Upper-endpoint DC Hurwitz) The DC matrix at the upper endpoint  $H:=\overline{A}_0+\overline{A}_1+B\gamma_2C$  is Hurwitz.

Then, for every delay  $\tau \geq 0$  the closed-loop system (21) is a positive system on  $\mathbb{R}^n_+$  and is globally exponentially stable from nonnegative histories.

The proof follows from the proofs of Theorems 2 and 3. *Note:* Due to space limitations, the region of attraction analysis regarding the  $\Gamma$ -set is not included here. A detailed treatment of this aspect can be found in our earlier work [21].

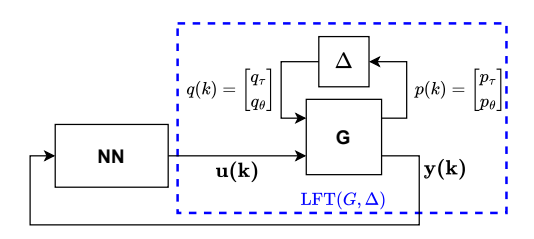


**Fig. 2:** Linear fractional transformation (LFT) model of the NN-feedback-loop with delay and interval uncetainty.

#### C. IQC-Based Method

In this subsection we adapt a state-of-the-art IQC framework for NN-in-the-loop verification [6] and tailor it to our risk model with delays and interval uncertainty to enable a fair comparison with our positivity-based approach. To align with [6] and to model delays in a rational state space filter, we work in discrete time and detail the necessary adaptations step by step. For completeness, the extension to continuous time is shortly outlined in a subsequent remark.

We expose the two uncertainty mechanisms—discrete delays and entrywise interval parametric uncertainty—through a single LFT interconnection as shown in 2. Denote by

$$p = \begin{bmatrix} p_{\tau} \\ p_{\theta} \end{bmatrix}, \qquad q = \begin{bmatrix} q_{\tau} \\ q_{\theta} \end{bmatrix}, \tag{22}$$

the stacked uncertainty port signals for delay  $(\tau)$  and interval  $(\theta)$ , respectively. The plant G is written in the standard form

$$x_{k+1} = A_G x_k + B_{G1} q_k + B_{G2} u_k,$$
  

$$p_k = C_G x_k + D_{G1} q_k + D_{G2} u_k,$$
  

$$u_k = \Phi(x_k) \text{ (optional controller)}.$$
(23)

The input-output relations of each uncertainty class are represented by an IQC. Specifically, the IQC is defined through a filter  $\Psi$  acting on the input p and output q, together with a constraint on the resulting signal r. The filter  $\Psi$  is described by the LTI system

$$\psi(k+1) = A_{\Psi}\psi(k) + B_{\Psi 1}p(k) + B_{\Psi 2}q(k), 
r(k) = C_{\Psi}\psi(k) + D_{\Psi 1}p(k) + D_{\Psi 2}q(k), 
\psi(0) = 0,$$
(24)

where  $\psi(k) \in \mathbb{R}^{n_{\psi}}$  is the filter state,  $r(k) \in \mathbb{R}^{n_r}$  is the output, and  $A_{\Psi}$  is Schur. All matrices are of compatible dimensions. A bounded, causal operator  $\Delta$  is said to satisfy the time-domain IQC associated with  $(\Psi, M)$  if, for all signals p and  $q = \Delta(p)$  and for all N, the prescribed inequality holds.

$$\sum_{k=0}^{N} r(k)^{\top} M r(k) \ge 0.$$
 (25)

We now specify all blocks in three steps. We define the blocks of delay, interval uncertainty, and their combination in turn.

## a) Delayed system LFT and IQC

Suppose there are  $\ell$  delay channels with integer delays  $d_i$ . For each  $i=1,\ldots,\ell$ ,

$$p_{\tau}^{(i)}(k) = \begin{bmatrix} x_k \\ u_k \end{bmatrix} \in \mathbb{R}^{n+m}, \quad q_{\tau}^{(i)}(k) = p_{\tau}^{(i)}(k - d_i) = \begin{bmatrix} x_{k-d_i} \\ u_{k-d_i} \end{bmatrix}$$

$$p_{\tau} = \text{col}(p_{\tau}^{(1)}, \dots, p_{\tau}^{(\ell)}) \in \mathbb{R}^{\ell(n+m)}, \quad q_{\tau} = \text{col}(q_{\tau}^{(1)}, \dots, q_{\tau}^{(\ell)}).$$

Write the nominal delayed plant without uncertainty as

$$x_{k+1} = A_0^c x_k + \sum_{i=1}^{\ell} A_i^c x_{k-d_i} + \sum_{i=1}^{\ell} B_i u_{k-d_i}, \qquad (26)$$

where the superscript  $^c$  in  $A_0^c$  and  $A_1^c$  denote the nominal (center) system without uncertainty. Place all nominal delayed terms into  $B_{G1,\tau}$  and generate  $p_{\tau}$  from (x,u) via

$$A_{G,\tau} = A_0^c, \quad B_{G1,\tau} = \begin{bmatrix} A_1^c & B_1 & \cdots & A_\ell^c & B_\ell \end{bmatrix}, \quad B_{G2,\tau} = 0$$

$$C_\tau = \mathbf{1}_\ell \otimes \begin{bmatrix} I_n \\ 0_{m \times n} \end{bmatrix}, \quad D_{G1,\tau} = 0, \quad D_{G2,\tau} = \mathbf{1}_\ell \otimes \begin{bmatrix} 0_{n \times m} \\ I_m \end{bmatrix}, \tag{27}$$

so that  $p_{\tau} = C_{\tau}x + D_{G2,\tau}u = \mathbf{1}_{\ell} \otimes \begin{bmatrix} x_k & u_k \end{bmatrix}^{\top}$ . Here  $\mathbf{1}_{\ell}$  is the  $\ell$ -vector of ones and  $\otimes$  denotes the Kronecker product.

## *IQC* for the delay

For each delay channel of size  $n_{\tau} = n + m$ , use the  $d_i$ -step delay-line filter

$$\psi_{k+1}^{(i)} = (J_{d_i} \otimes I_{n_{\tau}}) \psi_k^{(i)} + (e_1 \otimes I_{n_{\tau}}) p_{\tau}^{(i)}(k), 
r_{\tau}^{(i)}(k) = (e_{d_i}^{\top} \otimes (-I_{n_{\tau}})) \psi_k^{(i)} + I_{n_{\tau}} q_{\tau}^{(i)}(k),$$
(28)

with  $J_{d_i}$  the down-shift matrix,  $e_j$  the j-th standard basis vector, and  $\psi^{(i)} \in \mathbb{R}^{d_i n_\tau}$ . The hard time-domain IQC is

$$\sum_{k=0}^{N} (r_{\tau}(k))^{\top} M_{\tau} r_{\tau}(k) \ge 0, \qquad M_{\tau} = I, \qquad \forall N \ge 0, \quad (29)$$

where  $r_{\tau} = \text{col}(r_{\tau}^{(1)}, \dots, r_{\tau}^{(\ell)})$  with  $r_{\tau}^{(i)} = q_{\tau}^{(i)}(k)$  $p_{\tau}^{(i)}(k-d_i) \equiv 0$  satisfying exactly the equality in condition

#### b) Interval Uncertainty LFT and IOC

We expose the interval uncertainty as a separate port  $(p_{\theta}, q_{\theta})$ by moving the uncertainty part to an additive term  $E q_{\theta,k}$  as:

$$x_{k+1} = A_0^c x_k + \sum_{i=1}^{\ell} A_i^c x_{k-d_i} + \sum_{i=1}^{\ell} B_i u_{k-d_i} + E q_{\theta,k}.$$
 (30)

Rewrite  $[\underline{A}_0, \overline{A}_0]$  and  $[\underline{A}_1, \overline{A}_1]$  as affine/interval structure

$$A_0(\theta) = A_0^c + \sum_{i=1}^{s_0} \theta_{0j} \, \hat{A}_{0j}, \quad A_i(\theta) = A_i^c + \sum_{i=1}^{s_i} \theta_{ij} \, \hat{A}_{ij}, \ i = 1, ..., \ell,$$

with  $s_0, s_i$  being the number of independent scalar uncertainty channels to parametrize the uncertainty in  $A_0^c, A_i^c$ , and the independent scalars  $\theta_{ij}$  constrained in a box specified by an IQC as shown later. Collect all basis matrices in

$$E := \left[ \hat{A}_{0,1} \cdots \hat{A}_{0,s_0} \ \hat{A}_{1,1} \cdots \hat{A}_{\ell,s_{\ell}} \right] \in \mathbb{R}^{n \times ns_{\text{tot}}},$$

where  $s_{\text{tot}} := s_0 + \cdots + s_\ell$ , and form the signal that repeats

the appropriate state samples:

$$p_{\theta,k} = \operatorname{col}\left(\underbrace{x_k, \dots, x_k}_{s_0 \text{ times}}, \underbrace{x_{k-d_1}, \dots, x_{k-d_1}}_{s_1}, \dots, \underbrace{x_{k-d_\ell}, \dots, x_{k-d_\ell}}_{s_\ell}\right).$$
(31)

Let  $\Theta_k = \operatorname{diag}(\theta_{0,1}I_n, \dots, \theta_{\ell,s_\ell}I_n)$  and define

$$q_{\theta,k} = \Theta_k p_{\theta,k}$$
, so that  $x_{k+1} \leftarrow x_{k+1} + E q_{\theta,k}$ .

Thus, following (23), the updated blocks from (27) that generate  $p = \operatorname{col}(p_{\tau}, p_{\theta})$  and implement  $q = \operatorname{col}(q_{\tau}, q_{\theta})$  are

$$A_G = A_0^c$$
,  $B_{G1} = \begin{bmatrix} A_1^c & B_1 & \cdots & A_\ell^c & B_\ell & E \end{bmatrix}$ ,  $B_{G2} = 0$ ,

$$C_G = \begin{bmatrix} C_{\tau} \\ C_{\theta} \end{bmatrix}, \qquad D_{G1} = \begin{bmatrix} 0 \\ D_{\theta \leftarrow \tau} \end{bmatrix}, \quad D_{G2} = \begin{bmatrix} D_{G2,\tau} \\ 0 \end{bmatrix}, \quad (32)$$

 $A_{G,\tau}=A_0^c, \quad B_{G1,\tau}=\left[ \begin{array}{cccc} A_1^c & B_1 & \cdots & A_\ell^c & B_\ell \end{array} \right], \quad B_{G2,\tau}=0, \quad \text{where } C_\theta=\left[ \begin{array}{ccccc} \mathbf{1}_{s_0}\otimes I_n \\ \mathbf{0} \end{array} \right] \text{ stacks } x_k \text{ exactly } s_0 \text{ times, and } s_0 \in \mathbb{R}$  $D_{\theta \leftarrow \tau} = \mathbf{1}_{s_L} \overset{\mathsf{L}}{\otimes} \begin{bmatrix} I_n & \mathbf{0} \end{bmatrix}$  selects the delayed  $x_{k-d_i}$  components from each  $q_{\tau}^{(i)}$  and repeats them  $s_L = s_1 + \cdots + s_\ell$ times, in the same order as in (31).

# IQC for the interval block

We use a memoryless filter that outputs the pair  $(p_{\theta}, q_{\theta})$ directly, and a Symmetric Box multiplier.

$$\psi(k+1) = \mathbf{0},$$

$$r_{\theta}(k) = \mathbf{0}\psi(k) + \begin{bmatrix} \mathbf{I} \\ \mathbf{0} \end{bmatrix} p_{\theta}(k) + \begin{bmatrix} \mathbf{0} \\ \mathbf{I} \end{bmatrix} q_{\theta}(k).$$
(33)

Symmetric Box:  $q_{\theta} = \theta p_{\theta}$  with  $|\theta_j| \leq \rho_j$  gives

$$M_{\theta,j}(\rho_j) = \begin{bmatrix} \rho_j^2 I & 0\\ 0 & -I \end{bmatrix} \succeq 0.$$

Stack with nonnegative multipliers  $\mu_i \geq 0$ :

$$M_{\theta}(\mu) = \text{blkdiag}\left(\mu_1 M_{\theta,1}, \dots, \mu_{s_{\text{tot}}} M_{\theta,s_{\text{tot}}}\right) \succeq 0.$$
 (34)

c) Composite delay and interval LFT & IQC.

For constructing the combined IQC, let:

$$\Psi_{\Delta} = \text{blkdiag}(\Psi_{\tau}, \Psi_{\theta}) \qquad M_{\Delta} = \text{blkdiag}(M_{\tau}, M_{\theta}(\mu)).$$
 (35)

Define the extended state  $\zeta := \begin{bmatrix} x \\ \psi \end{bmatrix}$  . The assembly gives the extended realization

$$\zeta_{k+1} = A \zeta_k + B \begin{bmatrix} q_k \\ u_k \end{bmatrix}, \tag{36a}$$

$$r_k = C\zeta_k + D\begin{bmatrix} q_k \\ u_k \end{bmatrix}, \tag{36b}$$

$$A = \begin{bmatrix} A_G & 0 \\ B_{\Psi 1} C_G & A_{\Psi} \end{bmatrix}, \quad B = \begin{bmatrix} B_{G1} & B_{G2} \\ B_{\Psi 1} D_{G1} + B_{\Psi 2} & B_{\Psi 1} D_{G2} \end{bmatrix}$$
$$C = \begin{bmatrix} D_{\Psi 1} C_G & C_{\Psi} \end{bmatrix}, \quad D = \begin{bmatrix} D_{\Psi 1} D_{G1} + D_{\Psi 2} & D_{\Psi 1} D_{G2} \end{bmatrix}$$

where  $(A_{\Psi}, B_{\Psi}, C_{\Psi}, D_{\Psi})$  are those of  $\Psi_{\Delta}$ , and the columns of (B, C, D) are ordered consistently with  $q = \operatorname{col}(q_{\tau}, q_{\theta})$ .

**Theorem 5.** Consider the extended closed-loop system as in (36), and the composite IQC (35). If there exist P > 0, multipliers  $\mu_i \geq 0$ , and some  $\varepsilon > 0$  such that

$$\begin{bmatrix} A^{\top}PA - P & A^{\top}PB \\ B^{\top}PA & B^{\top}PB \end{bmatrix} + \begin{bmatrix} C \\ D \end{bmatrix} M_{\Delta} \begin{bmatrix} C & D \end{bmatrix} \leq -\varepsilon I, \quad (37)$$

then the origin is locally asymptotically stable for the given delays  $\{d_i\}$  and for all uncertainty realizations consistent with the interval box bounds. Moreover, every sufficiently small sublevel set  $\{\zeta: V(\zeta) \leq \rho\}$ , contained in the region where the IQCs are valid, is forward invariant.

*Proof.* Let  $V(\zeta) := \zeta^\top P \zeta$ . Left/right multiplying (37) by  $\begin{bmatrix} \zeta^\top & q^\top & u^\top \end{bmatrix}$  gives, at each time k,

$$V(\zeta_{k+1}) - V(\zeta_k) + r_k^{\top} (M_{\Delta}) r_k \le -\varepsilon \left\| \begin{bmatrix} \zeta_k \\ q_k \\ u_k \end{bmatrix} \right\|^2.$$

Summing from k = 0 to N yields

$$V(\zeta_{N+1}) - V(\zeta_0) + \sum_{k=0}^{N} \left( r_k^{\top}(M_{\Delta}) r_k \right) \le -\varepsilon \sum_{k=0}^{N} \left\| \begin{bmatrix} \zeta_k \\ q_k \\ u_k \end{bmatrix} \right\|^2.$$
 (38)

Since  $M_{\tau}, M_{\theta}(\mu) \succeq 0$  and  $V(.) \geq 0$ , letting  $N \to \infty$  gives  $\sum_{k=0}^{\infty} \left\| \left[ \zeta_k^{\top} \ q_k^{\top} \ u_k^{\top} \right]^{\top} \right\|^2 \leq V(\zeta_0)/\varepsilon < \infty$ , hence  $\left\| \left[ \zeta_k^{\top} \ q_k^{\top} \ u_k^{\top} \right]^{\top} \right\| \to 0$ . If  $V(\zeta) \leq \rho$  ensures the satisfaction of the IQCs, then  $V(\zeta_{k+1}) \leq V(\zeta_k)$  on the set, and for  $\rho$  small enough, the sublevel set is forward invariant.  $\square$ 

**Remark 1.** If an NN controller  $u = \pi(x)$  is included, its local-sector IQC is added as an extra quadratic term on the right-hand side of (37). A local sector IQC for FFNNs is presented in [6]. We shortly explain it below and utilize it to analyze the stability of delayed-uncertain NN feedback loops.

Neural network IQCs: Let  $\nu_{\phi}$  and  $\omega_{\phi} = \phi(\nu_{\phi})$  be the stacked inputs/outputs of all activations at the NN equilibrium  $(\nu^{\star}, \omega^{\star})$ . If the scalar activation  $\varphi$  satisfies local sector bounds  $[\alpha_{\phi}^{(i)}, \beta_{\phi}^{(i)}]$  on  $\nu_{\phi}^{(i)} \in [\underline{\nu}^{(i)}, \overline{\nu}^{(i)}]$  around  $\nu_{*}^{(i)}$ , as shown in 1 and stacked as  $(\alpha_{\phi}, \beta_{\phi})$ , then for any  $\lambda \in \mathbb{R}_{+}^{n_{\phi}}$ ,  $(n_{\phi} = n_{1} + n_{2} + \cdots + n_{q})$  summation of NN layer sizes),

$$\begin{bmatrix} \nu_{\phi} - \nu^{\star} \\ \omega_{\phi} - \omega^{\star} \end{bmatrix}^{\top} \Psi_{\phi}^{\top} M_{\phi}(\lambda) \Psi_{\phi} \begin{bmatrix} \nu_{\phi} - \nu^{\star} \\ \omega_{\phi} - \omega^{\star} \end{bmatrix} \ge 0, \tag{39}$$

$$\Psi_{\phi} = \begin{bmatrix} \operatorname{diag}(\beta_{\phi}) & -I_{n_{\phi}} \\ -\operatorname{diag}(\alpha_{\phi}) & I_{n_{\phi}} \end{bmatrix}, \quad M_{\phi}(\lambda) = \begin{bmatrix} 0_{n_{\phi}} & \operatorname{diag}(\lambda) \\ \operatorname{diag}(\lambda) & 0_{n_{\phi}} \end{bmatrix}.$$

These NN QCs are added to the composite IQC used for delays/uncertainty by simply adding an extra term  $R_{\phi}^{\top}\Psi_{\phi}^{\top}M_{\phi}(\lambda)\Psi_{\phi}R_{\phi}$  to the LMI (37). Here,  $R_{\phi}$  is the

 $R_{\phi}^{\top} \Psi_{\phi}^{\dagger} M_{\phi}(\lambda) \Psi_{\phi} R_{\phi} \quad \text{to the Livii (3.7).}$  selection matrix defined by  $R_{\phi} \begin{bmatrix} \zeta \\ q \\ u \end{bmatrix} = \begin{bmatrix} v_{\phi} - v^{\star} \\ w_{\phi} - w^{\star} \end{bmatrix}, \text{ with }$ 

detailed construction given in [6]. Notes on dimensions: (i) The delay filter has  $\sum_{i=1}^{\ell} d_i(n+m)$  states. (ii) The dimension of the interval filter is  $\sum_{i=1}^{s_{tot}} n^2$ . This can be reduced by introducing a low-dimensional basis that specifies how the uncertainty perturbs  $A_0$ ,  $A_i$ . However, such modeling couples the uncertainty channels and may exclude admissible elementwise variations. Thus, the elementwise channels adopted in this paper is the safest choice. Extension to continuous time: Use a rational delay approximation, e.g., Padé and its IQC to obtain an augmented rational LTI model, and replace the discrete-time Lyapunov condition in (37) with  $A^{T}P + PA$ ; the remaining steps are the same with minimal adaptations.

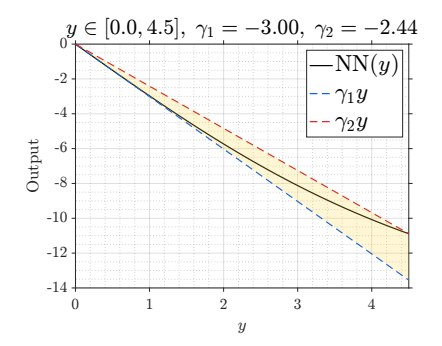


**Fig. 3:** Using (15), the local sector bounds over the  $\Gamma$ -set:  $y \in [0, 4.5]$  are calculated as  $\gamma_1 = -3$  and  $\gamma_2 = -2.44$ . As demonstrated  $\gamma_1 y \leq NN(y) \leq \gamma_2 y$ .

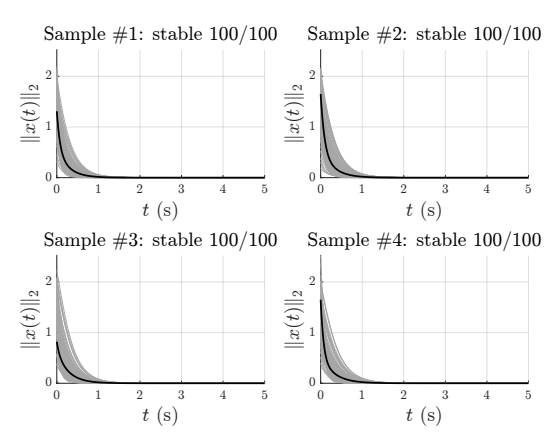


**Fig. 4:** Delay-free interval case with a trained NN controller. Four random plants are sampled from  $[\underline{A}_0,\overline{A}_0]$  and  $[\underline{A}_1,\overline{A}_1]$ . For each plant, 100 random initial conditions consistant with  $\Gamma$ -set  $(Cx_0 \in [0,4.5])$  are simulated; thin lines show  $\|x(t)\|_2$  and the bold line marks a representative (median) trajectory. Subplot titles report the proportion converging to zero.

## V. EXAMPLE

C1) Interval uncertainty only: To corroborate the positivity-based certificate, we choose an open-loop unstable interval

system (16) with 
$$\underline{A}_0 = \begin{bmatrix} -8 & 2 & 1 \\ 3 & -10 & 2 \\ 1 & 2 & -8 \end{bmatrix}$$
,  $\overline{A}_{0ij} = \underline{A}_{0ij} + 0.5$ ,  $\underline{A}_1 = 3\mathbf{1}\mathbf{1}^{\top}$ ,  $\overline{A}_1 = 3.5\mathbf{1}\mathbf{1}^{\top}$ ,  $B = \mathbf{1}$ ,  $C = \mathbf{1}^{\top}$ . We close the loop with our FFNN (zero biases) controller  $u = \phi(y)$  trained on trajectories of a PID  $(P = -0.9, I = -0.1, D = -0.2)$  controlled system. Using (15), the NN is calculated to lie in the sector  $[-3, -2.44]$  over the  $\Gamma$ -set:  $y \in [0, 4.5]$ . The sector bounds are shown in Fig. 3. System simulation results are demonstrated in Fig. 4. Consistent with Theorem 2,  $\underline{A} + B\gamma_1 C$  is Metzler and  $\overline{A} + B\gamma_2 C$  is Hurwitz and all trajectories decay to the origin.  $C2$ ) Delay only: We now consider the delayed Lur'e system

- (17) with  $A_0 = \underline{A}_0$  as above,  $A_1 = 3 \, \mathbf{1} \mathbf{1}^{\top}$ ,  $B = \mathbf{1}$ ,  $C = \mathbf{1}^{\top}$ , and the same trained NN controller. With  $A_0$  being Metzler,  $B, C, A_1 + B\gamma_1 C \geq 0$ , and  $A_0 + A_1 + B\gamma_2 C$  being Hurwitz, Theorem 3 predicts exponential stability. Fig. 5 shows the simulation results are consistent with the expectation.
- C3) Combined delay & interval uncertainty: To illustrate the combined-delay/uncertainty case, we draw 5 random plants by sampling  $(A_0, A_1)$  uniformly from the interval box of the example C1 and 5 random delays from  $\tau \in [0.2, 3.0]$  s.

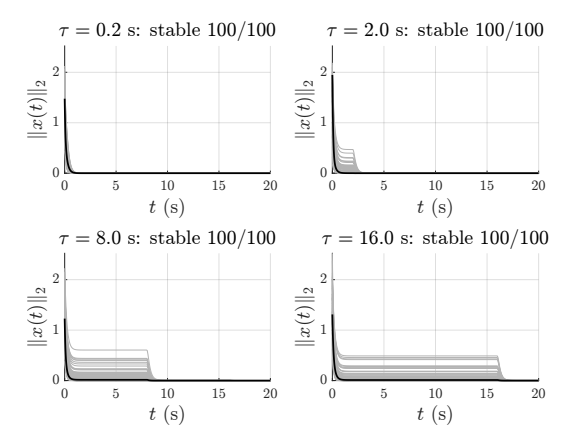
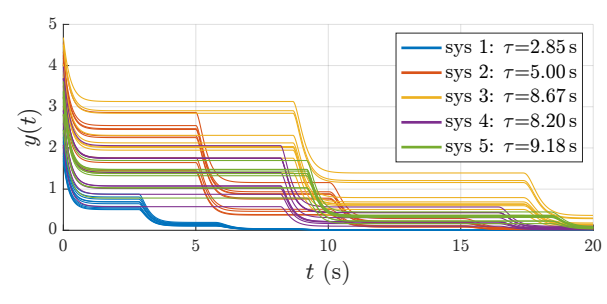


Fig. 5: Delay-only case with the trained NN controller. Four tiles correspond to  $\tau \in \{0.2, 2, 8, 16\}$  s. For each delay, 100 random constant histories  $x(t) \equiv x_0$  on  $[-\tau, 0]$  with  $x_0 \sim \text{Unif}([-1.5, 1.5]^3)$  are simulated. Thin curves plot  $||x(t)||_2$ ; the bold curve marks a representative (median) trajectory. Subplot titles report the proportion converging to zero.



**Fig. 6:** Outputs y(t) = Cx(t) for five sampled  $(A_0, A_1, \tau)$  systems; simulated ten positive initial conditions  $(y_0 \in [0, 4.5])$  per system.

For all sampled systems, the conditions of Theorem 4 is satisfied as outlined in examples C1 and C2. As shown in Fig. 6, For each sampled system we simulate from 10 random constant histories  $x_h(t) \equiv x_0$  inside  $\Gamma$ -set with the trained NN controller. We distinguish systems with different colors. Across the sampled cases the output trajectories contract toward zero, empirically supporting Theorem 4.

IOC comparison: The IOC-based method is also run for two different discretization/delay configurations of the same interval system outlined in example C1, within the same  $\Gamma$ -set. As shown in Table I, the IQC-based method is delay/configuration dependent (cannot certify in cases) and performs up to  $10^5 \mathbf{X}$  slower. Further comparison notes are explained in Table II.

## VI. CONCLUSION

We present a positivity-based, scalable safety-verification framework for autonomous systems with NN controllers subject to two risk sources: time delay and interval-matrix uncertainty. A novel local sector bound for FFNNs underpins linear, delay-independent certificates. We benchmark against a state-of-the-art IQC-based method and, in simulations, achieve faster runtimes while certifying cases the benchmark cannot. Future work will extend the approach to additional risk models and to other NN architectures (e.g., RNNs).

#### REFERENCES

[1] Z. Du, H. Balim, S. Oymak, and N. Ozay, "Can transformers learn optimal filtering for unknown systems?," *IEEE Control Systems Letters*, vol. 7, pp. 3525–3530, 2023.

**TABLE I:** effect of discretization & delay on verification runtime.

Discretization step(s)	Delay(s)	IQC runtime(s)	Positivity runtime(s)
0.1	0.7	cannot certify 2.22	$5.3 \times 10^{-5}$
0.01	0.07		$5.6 \times 10^{-5}$

**TABLE II:** Method characteristics.

	Positivity-based	IQC-based
Certificate Solve class variables Dimension	Metzler/Hurwitz Linear constraints Few (structure-exploiting)  n	$\begin{array}{c} \text{Lyapunov + IQCs} \\ \text{SDP} \\ \text{grows with filters/NN/delays} \\ n(1+d_i) + n_\phi + \sum_{i=1}^{stot} n^2 \end{array}$

M. Sznaier, A. Olshevsky, and E. D. Sontag, "The role of systems theory in control oriented learning," in 25th International Symposium on Mathematical Theory of Networks and Systems, 2022.

[3] M. Fazlyab, M. Morari, and G. J. Pappas, "Safety verification and robustness analysis of neural networks via quadratic constraints and

robustness analysis of neural networks via quadratic constraints and semidefinite programming," *IEEE Transactions on Automatic Control*, vol. 67, no. 1, pp. 1–15, 2020.

Z. Qin, K. Zhang, Y. Chen, J. Chen, and C. Fan, "Learning safe multiagent control with decentralized neural barrier certificates," *arXiv preprint arXiv:2101.05436*, 2021.

C. Dawson, S. Gao, and C. Fan, "Safe control with learned certificates: A survey of neural lyapunov, barrier, and contraction methods for robotics and control," *IEEE Transactions on Robotics*, vol. 39, no. 3, pp. 1749–1767 2023 p. 1749–1767, 2023.

[6] H. Yin, P. Seiler, and M. Arcak, "Stability analysis using quadratic constraints for systems with neural network controllers," *IEEE Trans*-

actions on Automatic Control, vol. 67, no. 4, pp. 1980–1987, 2021. W. Xiang, H.-D. Tran, and T. T. Johnson, "Output reachable set estimation and verification for multilayer neural networks," *IEEE* transactions on neural networks and learning systems, vol. 29, no. 11,

[8] G. Singh, T. Gehr, M. Püschel, and M. Vechev, "An abstract domain for certifying neural networks," *Proceedings of the ACM on Programming Languages*, vol. 3, no. POPL, pp. 1–30, 2019.
[9] H. Zhang, T.-W. Weng, P.-Y. Chen, C.-J. Hsieh, and L. Daniel, "Efficient neural network robustness certification with general activation functions," *Advances in neural information processing systems*, vol. 31, 2018.

[10] M. Everett, G. Habibi, and J. P. How, "Efficient reachability analysis of closed-loop systems with neural network controllers," in 2021 IEEE International Conference on Robotics and Automation (ICRA), pp. 4384–4390, IEEE, 2021.

[11] J.-P. Richard, "Time-delay systems: an overview of some recent advances and open problems," automatica, vol. 39, no. 10, pp. 1667–

1694, 2003.

[12] K. Gu, V. L. Kharitonov, and J. Chen, "Stability of time-delay systems," *IEEE Control Systems*, vol. 24, no. 4, pp. 104–104, 2004.
[13] W. Sun, Y. Wu, and X. Lv, "Adaptive neural network control for a control of the contro W. Sun, Y. Wu, and A. Lv, Adaptive neural network control for full-state constrained robotic manipulator with actuator saturation and time-varying delays," *IEEE Transactions on Neural Networks and Learning Systems*, vol. 33, no. 8, pp. 3331–3342, 2021.

Z. Sadat Aghayan, A. Alfi, Y. Mousavi, and A. Fekih, "Robust delay-time of the partiable fractional.

[14] Z. Sadaĭ Aghayan, A. Alfi, Y. Mousavi, and A. Fekih, "Robust delay-dependent output-feedback pd controller design for variable fractional-order uncertain neutral systems with time-varying delays," *IEEE Transactions on Systems, Man, and Cybernetics: Systems*, vol. 55, no. 3, pp. 1986–1996, 2025.
[15] C. Yuan and F. Wu, "Dynamic iqc-based control of uncertain lft systems with time-varying state delay," *IEEE Transactions on Cybernetics*, vol. 46, no. 12, pp. 3320–3329, 2016.
[16] V. K. Shukla, M. C. Joshi, P. K. Mishra, Y. Mousavi, M. R. Zadeh, and A. Fekih, "Predefined synchronization of mixed and leakage-delayed.

A. Fekih, "Predefined synchronization of mixed and leakage-delayed

quaternion-valued neural network," *International Journal of Dynamics and Control*, vol. 13, no. 2, p. 51, 2025.
[17] L. Farina and S. Rinaldi, *Positive linear systems: theory and applica-*

[17] L. Farina and S. Kinaldi, Positive linear systems: theory and applications. John Wiley & Sons, 2011.
[18] B. Shafai, A. Oghbaee, and T. Tanaka, "Positive stabilization with maximum stability radius for linear time-delay systems," in 53rd IEEE Conference on Decision and Control, pp. 1948–1953, IEEE, 2014.
[19] A. Bill, C. Guiver, H. Logemann, and S. Townley, "Stability of nonnegative lur'e systems," SIAM Journal on Control and Optimization, vol. 54, no. 3, pp. 1176–1211, 2016.
[20] H. Montazeri Hedesh and M. Siami, "Ensuring both positivity and stability using sector-bounded nonlinearity for systems with neural

stability using sector-bounded nonlinearity for systems with neural network controllers," *IEEE Control Systems Letters*, vol. 8, pp. 1685–

[21] H. M. Hedesh, M. K. Wafi, and M. Siami, "Local stability and region of attraction analysis for neural network feedback systems under positivity constraints," arXiv preprint arXiv:2505.22889, 2025.